Power law correlations for the lift force on a particle in plane Poiseuille flow

J. Wang and D. D. Joseph
University of Minnesota, July 12, 2002

Abstract

The lift force on a circular particle in plane Poiseuille flow is studied by numerical simulation. We obtain the lift force as a function of the distance from the centerline of the particle to the wall. This function can be divided into stable and unstable equilibrium branches. The results show the existence of four different branches between the wall and the centerline, with the following order: wall – stable – unstable – stable – unstable – centerline, meaning that the branch close to the wall is stable, while the branch close to the centerline is unstable.

The lift force is determined by the relative motion between the particle and its surrounding fluid. Joseph and Ocando (2002) found that the relative motion can be characterized by the slip velocity and the angular slip velocity discrepancy. By numerical simulation, the slip velocity and the angular slip velocity discrepancy are also obtained as functions of the distance from the centerline of the particle to the wall. Correlations for the lift force are then derived in terms of the slip velocity and the angular slip velocity discrepancy. Using dimensionless parameters, the correlation is a power law for the stable branch near the wall and a linear relation (which can be taken as a power law with the power of one) for the stable branch near the centerline. The correlations are compared to analytical expressions for lift force in the literature and we believe that the correlations capture the essence of the mechanism of the lift force.

1.Introduction:

There are many studies of the lifting of free particles in shear flow. A fairly complete recent list of references can be found in Patankar, Huang, Ko and Joseph (2001a) and Joseph and Ocando (2002). Different analytical expressions for the lift force can be found in the literature. Auton (1987) gave a formula for the lift on a particle in an inviscid fluid in which uniform motion is perturbed by a weak shear. Bretherton (1962) found an expression for the lift per unit length on a cylinder (two-dimensional sphere) in an unbounded linear shear flow at small values of Reynolds number. Saffman (1965, 1968) gave an expression for the lift on a sphere in an unbounded linear shear flow. Saffman's equation is in the form of the slip velocity multiplied by a factor, which can be identified as a density multiplied by a circulation as in the famous formula

$\rho U\Gamma$ for aerodynamic lift. A number of formulas like Saffman's exist and a review of such formulas can be found in McLaughlin (1991).

Segrè and Silberberg (1961, 1962) studied the migration of dilute suspensions of neutrally buoyant spheres in pipe flows. The particles migrate away from the wall and centerline and accumulate at 0.6 of a pipe radius. Formulas like Saffman's can not explain the Segrè and Silberberg effect because they can not account for the migration away from both the wall and the centerline.

Ho and Leal (1974) analyzed the motion of a neutrally buoyant particle in both simple shear flow and plane Poiseuille flows. They found that for Couette flow, the equilibrium position is the centerline, whereas for Poiseuille flow, it is 0.6 of the channel half-width from the centerline which is in good agreement with Segrè and Silberberg (1961, 1962). To understand the Segrè and Silberberg effect, the effect of the curvature of the undisturbed velocity profile was found to be important. Details of the theoretical analysis of lift can be found in Vasseur and Cox (1976), Schonberg and Hinch(1989), and Asmolov (1999).

Joseph and Ocando (2002) analyzed the role of the slip velocity and the angular slip velocity on migration and lift. The angular slip velocity is defined as $\Omega_s = \Omega_p - \Omega_f = \Omega_p + \dot{\gamma}/2$, where $(-\dot{\gamma}/2)$ is the angular velocity of the fluid at a point where the shear rate is $\dot{\gamma}$ and Ω_p is the angular velocity of the particle. They showed that the discrepancy between the angular slip velocity of a migrating particle and the angular slip velocity at its equilibrium position, $\Omega_s - \Omega_{se}$, is the quantity that changes sign above and below the equilibrium position. Thus, this discrepancy can be used to account for the migration from both the wall and the centerline to the equilibrium position.

In this paper we focus on the lift force on a single particle in plane Poiseuille flow. Joseph and Ocando (2002) pointed out qualitatively the lift force is proportional to the product of the slip velocity and the angular slip velocity discrepancy. In the present paper, quantitative expressions for the lift force in terms of the slip velocity and the angular slip velocity discrepancy are obtained using the method of correlations.

The method of correlations applied to real or to numerical experiments is a way to derive formulae and analytic expressions from the processing of data. A famous example of the success of the method of correlations is the Richardson-Zaki correlation (1954) which is obtained by processing the data of fluidization experiments. Richardson-Zaki correlation describes the

complicated dynamics of fluidization by drag and is widely used for modeling the drag force on particles in solid-liquid mixtures.

The method of correlations has been heavily used in our studies of solid-liquid flows. From numerical data, we have drawn power law correlations for single particle lift and for the bed expansion of many particles in slurries (Patankar *et al.* 2001a; Choi and Joseph 2001; Patankar, Ko, Choi, and Joseph 2001b). The prediction of the power laws for proppant transport from numerical simulation is verified by the engineering correlations obtained from experimental data in Patankar, Joseph, Wang, Barree, Conway and Asadi (2002) and Wang, Joseph, Patankar, Conway and Barree (2002). The existence of such power laws is an expression of self-similarity, which has not yet been predicted from analysis or physics. The flow of dispersed matter appears to obey those self-similar rules to a large degree (Barenblatt 1996).

2. Governing equations and numerical methods:

The numerical methods used here is described in Joseph (2000), Choi and Joseph (2001) and Patankar *et al.* (2001a) and will not be described in detail here. Suffice to say that the method is based on unstructured body-fitted moving grids (ALE method). The two-dimensional computational domain is shown in figure 1. l and W are the length and width of the channel respectively, and d is the diameter of the particle. The simulation is performed with a periodic boundary condition in the x-direction. The solutions are essentially independent of the channel length l for sufficiently large l. The geometric parameters are W/d = 12, l/d = 22 where d = 1cm. The values of these parameters are taken from Patankar *et al.* (2001a) where they justified that the solutions are essentially independent of the selected geometric parameters. A constant pressure gradient $-\overline{p}$ is applied which gives rise to Poiseuille flow.

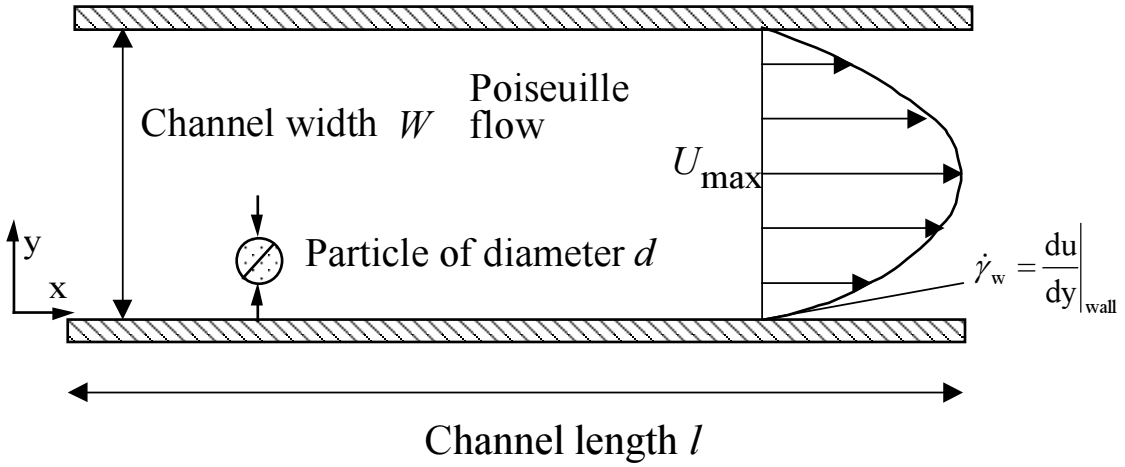

Figure 1:The two-dimensional rectangular computational domain.

The governing equation for the fluid is the Navier-Stokes equations:

$$\rho_f\left(\frac{\partial \mathbf{u}}{\partial t}+(\mathbf{u}\cdot\nabla)\mathbf{u}\right)=-\nabla P+\rho_f\mathbf{g}+\eta\nabla^2\mathbf{u} \tag{2.1}$$

where ρ_f is the fluid density which is 1g/cc in our simulations. $\mathbf{u}(\mathbf{x},t)$ is the fluid velocity, $P(\mathbf{x},t)$ is the pressure, η is the viscosity of the fluid, and $\mathbf{g}$ is the gravitational acceleration and $\mathbf{g}=-g\mathbf{e}_\mathbf{y}$, where $\mathbf{e}_\mathbf{y}$ is the unit vector in the y-direction.

The motion of solid particles satisfies Newton's law:

$$\begin{aligned} m\frac{d\mathbf{U}_p}{dt}&=m\mathbf{g}+\oint[-P\mathbf{1}+\mathbf{T}]\cdot\mathbf{n}d\Gamma,\\ \frac{d(\mathbf{I}\cdot\mathbf{\Omega}_\mathbf{p})}{dt}&=\oint(\mathbf{x}-\mathbf{X})\times([-P\mathbf{1}+\mathbf{T}]\cdot\mathbf{n})d\Gamma \end{aligned} \tag{2.2}$$

where m is the mass of the particle, $\mathbf{I}$ is the moment of inertia tensor, $\mathbf{U}_p$ is the translational velocity, $\mathbf{\Omega}_\mathrm{p}$ is the angular velocity, and $\mathbf{X}$ is the coordinate of the center of mass of the particle. We consider circular particles of diameter d with the mass per unit length $m = \rho_p\pi d^2/4$ and the moment of inertia per unit length $I = \rho_p\pi d^4/32$. The particle density ρ_p enters this problem through the buoyant weight (3.1) and as a factor in the left side of (2.2) which vanishes in steady flow. The no-slip condition is imposed on the particle boundaries:

$$\mathbf{u}=\mathbf{U}_\mathrm{p}+\mathbf{\Omega}_\mathrm{p}\times(\mathbf{x}-\mathbf{X}). \tag{2.3}$$

The pressure is split as following:

$$\begin{aligned} P&=p+\rho_f\mathbf{g}\cdot\mathbf{x}-\bar{p}\mathbf{e}_x\cdot\mathbf{x},\\ \nabla P&=-\nabla p-\rho_f\mathbf{g}+\bar{p}\mathbf{e}_\mathrm{x} \end{aligned} \tag{2.4}$$

where $\mathbf{e}_\mathbf{x}$ is the unit vector in the x-direction. The applied pressure gradient term then appears as a body force and p is solved in the simulation.

We refer Poiseuille flow without particles as the basic flow. The velocity profile of the basic flow is given by: $u(y)=(\bar{p}/2\eta)(W-y)y$. Flows are indexed by a Reynolds number

$$R=\frac{\rho_f\dot{\gamma}_w d^2}{\eta} \tag{2.5}$$

based on the wall shear rate $\dot{\gamma}_w = (\overline{p}/2\eta)W$.

3. Stable and unstable equilibrium regions:

An equilibrium is achieved for a freely moving and rotating circular particle with a given density in Poiseuille flow when the particle migrates to a position *ye* of steady rectilinear motion in which the acceleration and angular acceleration vanish and the hydrodynamic lift just balances the buoyant weight. Two types of simulations are performed, **unconstrained simulation** and **constrained simulation**. In unconstrained simulations, a particle is allowed to move and rotate freely to migrate to its equilibrium position. The initial translational and angular velocities of the particle are prescribed and initial-value problems are solved to obtain the equilibrium state. In constrained simulations, the position of the particle in the y-direction y_p is fixed and the particle is allowed to move in x-direction and rotate. The solution of the flow evolves dynamically to a steady state at which the lift force per unit length L on the particle is computed. Such a steady state will be an equilibrium at $y=y_p$ if the density of the particle is selected so that L just balances the buoyant weight per unit length, satisfying:

$$L = (\rho_p - \rho_f) g \frac{\pi d^2}{4}. \tag{3.1}$$

From steady solutions of constrained simulations, we are able to obtain L on the particle at any position y in the channel. We can divide the curve of L vs. y from the wall to the centerline into four branches by three "turning points" (see figure 2). The "turning point" is defined as the position where the slope of the L vs. y curve is zero. On the first and third branches of steady solutions, the slope of L vs. y curve is positive, and the equilibrium points on these branches are stable. On the second and fourth branches of steady solutions, the slope of L vs. y curve is negative, and the equilibrium points are unstable. We will indicate the unstable branches by dotted lines in the figures.

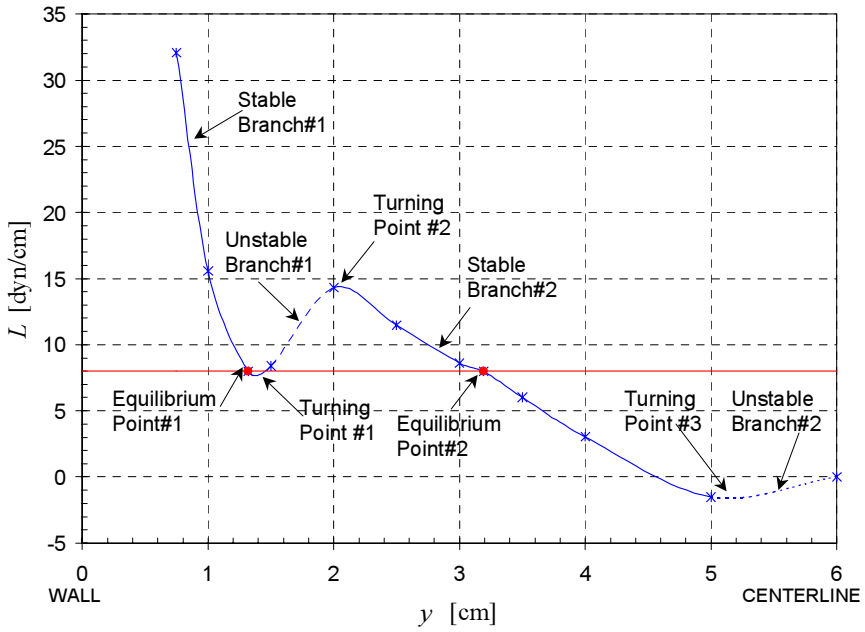

Figure 2. A plot of L vs. y for R=20 from constrained simulations. The stable and unstable branches and three turning points are illustrated. Unstable branches are indicated by dotted lines. Two stable equilibrium points for a particle with $\rho_p = 1.01\rho_f$ *are shown.*

From the L vs. y curve, the equilibrium position for a particle with a certain ρ_p can be determined. The lift force required to balance the buoyant weight of a particle can be computed from (3.1). If we draw a line on which L equals to this required lift force, the points of intersections between this line and the L vs. y curve are the equilibrium points for this particle. For heavier-than-fluid particles with certain densities, there exist multiple stable equilibrium positions from the wall to the centerline (see figure 2 where two stable equilibrium points for a particle with $\rho_p = 1.01\rho_f$ are shown). However, for a neutrally buoyant particle (L=0), only one stable equilibrium point exists from the wall to the centerline.

Ho and Leal (1974) showed that the equilibrium position of a neutrally buoyant freely moving and rotating sphere is between the wall and the centerline. They assumed that the plane bounding walls were so closely spaced that the lift could be obtained by perturbing Stokes flow with inertia. They calculated dimensionless lateral force vs. lateral position curves (equivalent to our L vs. y curve) for simple shear flow and two-dimensional Poiseuille flow which are shown in figure 3. Comparing the dashed line in figure 3 which is for two-dimensional Poiseuille flow and the L vs. y curve in figure 2, one can see that both of the two plots imply the centerline is an unstable equilibrium position. However, the dashed line in figure 3 indicates that there are two

branches from the wall to the centerline: wall – stable – unstable – centerline, whereas four branches exist according to figure 2. Ho and Leal only considered neutrally buoyant particle and did not include the gravity term in the governing equation used in their calculation. The frame of their work did not enable them to study the multi-equilibrium positions of heavier-than-fluid particles. The results shown in figure 2 and 3 are not strictly comparable; Ho and Leal studied spheres (3D) between plane walls at indefinitely small R whereas our calculation is for 2D particles at much higher Reynolds numbers.

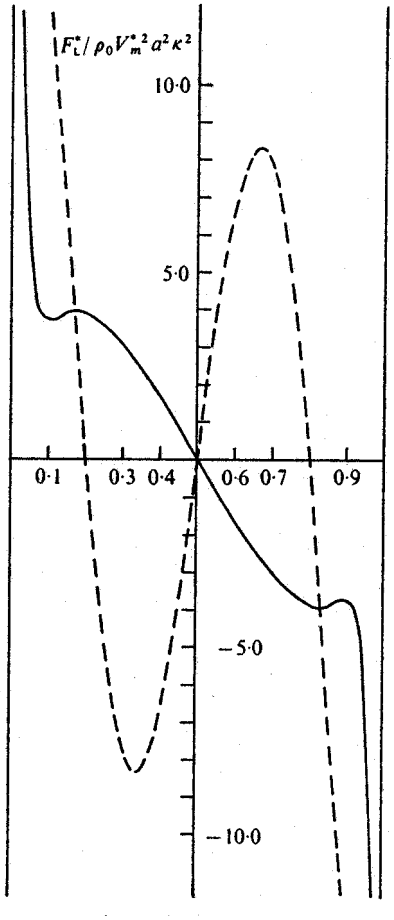

Figure 3.Lateral force as a function of lateral position, both in dimensionless form. —-, simple shear flow; - - -, 2D Poiseuille flow. (Adapted from Ho and Leal 1974)

The distinction between stable and unstable equilibrium is essential to understand the mechanism of the lift. Joseph and Ocando (2002) showed that the angular slip velocity discrepancy Ω_s -Ω_{se} has the same sign as the lift force across a stable equilibrium position, in contrast, the discrepancy has the opposite sign as the lift force across an unstable equilibrium

position. Correlations between the lift force and the slip velocities are achieved only on the stable branches of steady solution.

4.Lift correlations

The lift force on a particle in a shear flow is determined by the relative motion between the particle and its surrounding fluid. Joseph and Ocando (2002) showed that the relative motion can be characterized by the slip velocity $U_s = U_f - U_p$ and the angular slip velocity discrepancy $\Omega_s - \Omega_{se}$. Joseph and Ocando (2002) proposed that $L = CU_s\Gamma_s$ where $\Gamma_s \propto \Omega_s - \Omega_{se}$. In the present paper, we determine the constant C using the method of correlations. The correlation is a power law for the stable branch of steady solutions near the wall and a linear relation for the stable branch of steady solutions near the centerline.

The analysis of the equilibrium of a neutrally buoyant or heavier-than-fluid particle can be framed in a uniform way by looking for the equilibrium position where the net force Λ on the particle vanishes:

$$\Lambda = L - (\rho_p - \rho_f)g\pi d^2/4 = 0 . \qquad (4.1)$$

For the particle to migrate to its equilibrium position, the net force Λ must change sign across the equilibrium position. Joseph and Ocando (2002) showed that $\Omega_s - \Omega_{se}$ is the quantity that changes sign above and below the equilibrium position. We summarize the correlation between $\Omega_s - \Omega_{se}$ and Λ for the neutrally buoyant and heavier-than-fluid particles as following: $\Omega_s - \Omega_{se} > 0$ when the particle is below the equilibrium position and $\Omega_s - \Omega_{se} < 0$ when the particle is above the equilibrium position. Across a stable equilibrium position, negative $\Omega_s - \Omega_{se}$ leads to negative Λ, positive $\Omega_s - \Omega_{se}$ leads to positive Λ; across an unstable equilibrium position, negative $\Omega_s - \Omega_{se}$ leads to positive Λ, positive $\Omega_s - \Omega_{se}$ leads to negative Λ.

Motivated by the conclusion that the sign of $\Omega_s - \Omega_{se}$ is the same with the sign of Λ across a stable equilibrium position, we seek the correlations between L and the product $U_s \cdot (\Omega_s - \Omega_{se})$. L, U_s and Ω_s can all be computed as functions of y by constrained simulation which is independent of ρ_p. As an example, figure 4 shows the relative values of L, U_s and Ω_s at R=20.

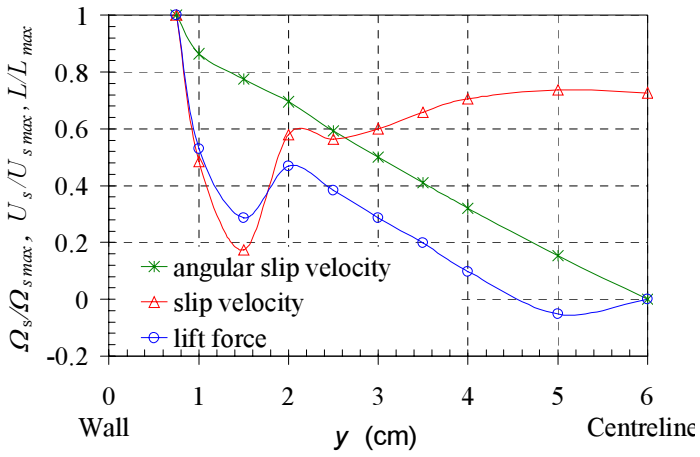

Figure 4. L(y), U_s(y) and Ω_s(y) computed by constrained simulation at R=20.

Local dimensionless parameters which depend on y are used to express the correlations between L and $U_s \cdot (\Omega_s - \Omega_{se})$. The local dimensionless net force is:

$$\lambda(y) = \frac{4\rho_f d\left[L(y) - (\rho_p - \rho_f)g\pi d^2/4\right]}{\pi\eta^2} \tag{4.2}$$

Two local Reynolds numbers are based on U_s and Ω_s -Ω_{se} respectively:

$$R_U(y) = \frac{\rho_f U_s(y) d}{\eta} \tag{4.3}$$

$$R_\Omega(y) = \frac{\rho_f [\Omega_s(y) - \Omega_{se}] d^2}{\eta} \tag{4.4}$$

The correlations between L and $U_s \cdot (\Omega_s - \Omega_{se})$ can be expressed as the correlations between λ and $(R_U \cdot R_\Omega)$. We define the product of R_U and R_Ω as F:

$$F(y) = R_U \cdot R_\Omega = \frac{\rho_f^2 U_s(y)[\Omega_s(y) - \Omega_{se}]d^3}{\eta^2} \tag{4.5}$$

To derive the correlations between λ(y) and F(y), a stable equilibrium position need to be chosen as the reference. Recall the L vs. y curve, every point on the stable branches of steady solutions at a given y is a possible equilibrium for a certain ρ_p and is a candidate for the reference position. We present two forms of the correlations, one with the single equilibrium position of a neutrally buoyant particle as the reference, the other with the multi-equilibrium positions of a heavier-than-fluid particle as the references.

4.1 Correlations with the single equilibrium position of a neutrally buoyant particle as the reference

For a neutrally buoyant particle, a single equilibrium position exists at $y = y_e^N$ (the superscript is for "neutral") with:

$$L(y_e^N) = 0 \text{ and } \Omega_s(y_e^N) = \Omega_{se}^N .$$

Considering $\rho_p = \rho_f$, the dimensionless parameters have the following form:

$$\lambda(y) = \frac{4\rho_f dL(y)}{\pi\eta^2} \text{ and } F(y) = \frac{\rho_f^2 U_s(y)\left[\Omega_s(y) - \Omega_{se}^N\right]d^3}{\eta^2} .$$

From our simulation, the equilibrium position of a neutrally buoyant particle is always on the stable branch of steady solutions near the centerline. *L(y)* and $\Omega_s(y) - \Omega_{se}^N$ are positive at every point on the stable branch of steady solutions near the wall; *L(y)* and $\Omega_s(y) - \Omega_{se}^N$ change sign across y_e^N on the stable branch of steady solutions near the centerline. Hence, in this section, we will refer the stable branch of steady solutions near the wall as the stable branch of steady solutions away from equilibrium, and the stable branch of steady solutions near the centerline as the stable branch of steady solutions through equilibrium. It should be emphasized that the lift force *L* is obtained from the steady solutions from constrained simulations and does not depend on ρ_p. Therefore, the correlations apply to both neutrally buoyant particles and heavier-than-fluid particles even though the equilibrium of a neutrally buoyant particle is chosen as the reference.

We find that the correlation between $\lambda(y)$ and $F(y)$ is a power law on the stable branch of steady solutions away from equilibrium and a linear relation on the stable branch of steady solutions through equilibrium.

$\lambda(y) = aF(y)^m$ on the stable branch of steady solutions away from equilibrium; (4.6)

$\lambda(y) = kF(y)$ on the stable branch of steady solutions through equilibrium. (4.7)

The correlations are derived for Poiseuille flows with the Reynolds number R = 10, 20 and 40. In figure 5, the correlations for the stable branch of steady solutions away from equilibrium are plotted. It can be seen that power laws fit the data well. Following are the power law correlations along with the correlation coefficients σ^2.

$$\lambda(y) = 17.94F(y)^{0.400}, \ \sigma^2=0.999, \ R=10; \quad (4.8)$$

$$\lambda(y) = 27.29F(y)^{0.411}, \ \sigma^2=0.986, \ R=20; \quad (4.9)$$

$$\lambda(y) = 38.01F(y)^{0.448},\ \sigma^2=0.995,\ R=40. \tag{4.10}$$

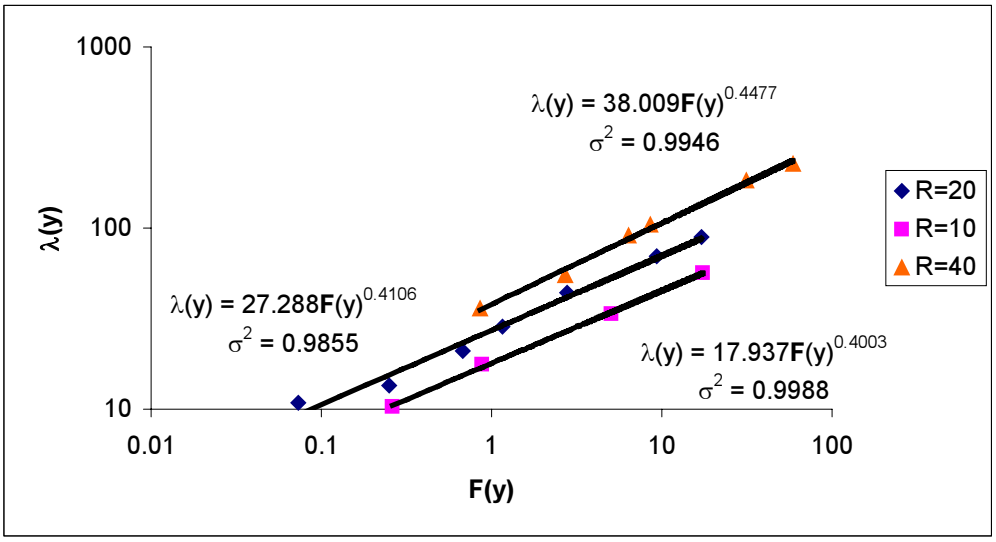

Figure 5 The power law correlations between λ(y) and F(y) for the stable branch of steady solutions away from equilibrium in the flows with R = 10, 20 and 40.

In figure 6, the linear correlation between $\lambda(y)$ and $F(y)$ for the stable branch of steady solutions through equilibrium in the flow with R=20 is plotted. The plots for flows with R=10 and 20 are skipped whereas the linear equations along with the correlation coefficients are listed below.

$$\lambda(y) = 53.17F(y),\ \sigma^2=0.983,\ R=10; \tag{4.11}$$

$$\lambda(y) = 30.74F(y),\ \sigma^2=0.990,\ R=20; \tag{4.12}$$

$$\lambda(y) = 24.35F(y),\ \sigma^2=0.999,\ R=40. \tag{4.13}$$

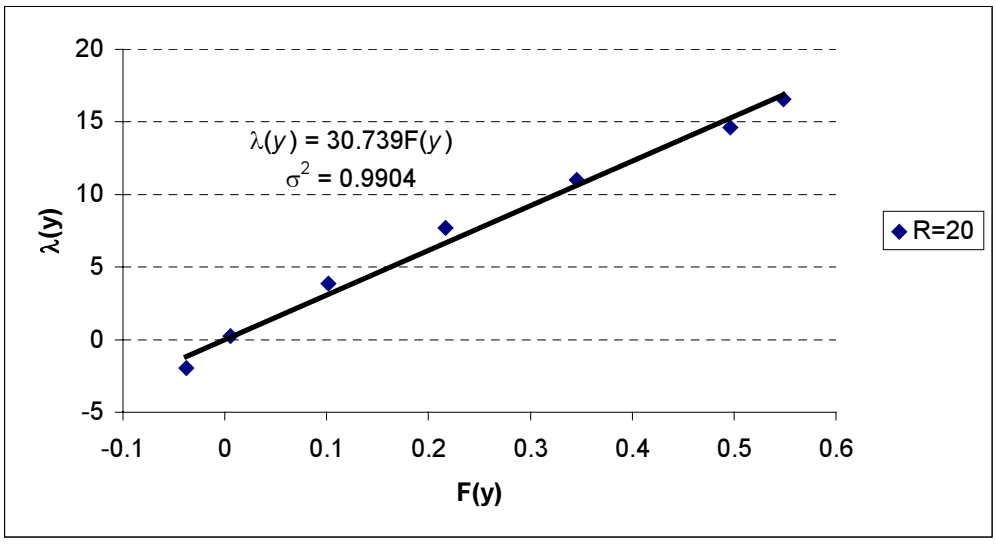

Figure 6. The linear correlation between λ(y) and F(y) for the stable branch of steady solutions through equilibrium in the flow with R=20.

It is noticed that the prefactor *a* and the exponent *m* in the power law correlations and the slope *k* in the linear correlations are functions of the Reynolds number *R*. In table 1, these coefficients are listed.

R	*a*	*m*	*k*
10	17.94	0.400	53.17
20	27.29	0.411	30.74
40	38.01	0.448	24.35

Table 1.The prefactor a, the exponent m and the slope k as functions of the Reynolds number R.

We plot *a*, *m* and *k* as functions of *R* in figures 7, 8 and 9 respectively.

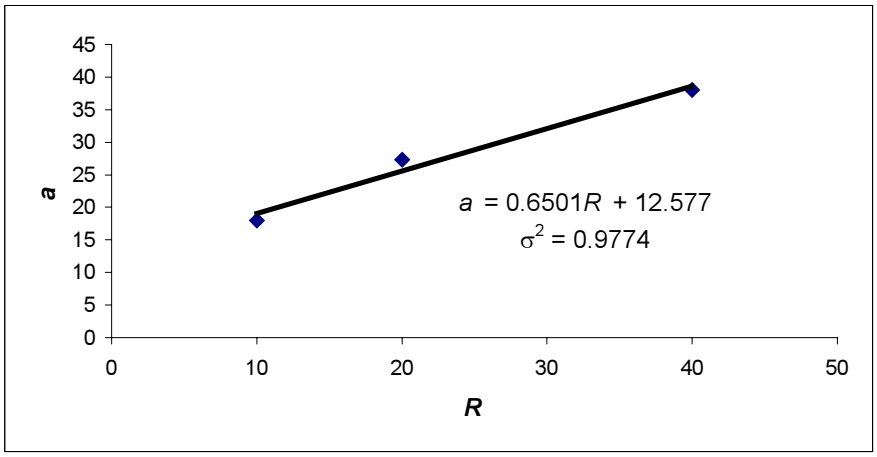

Figure 7. The prefactor a vs. the Reynolds number R..

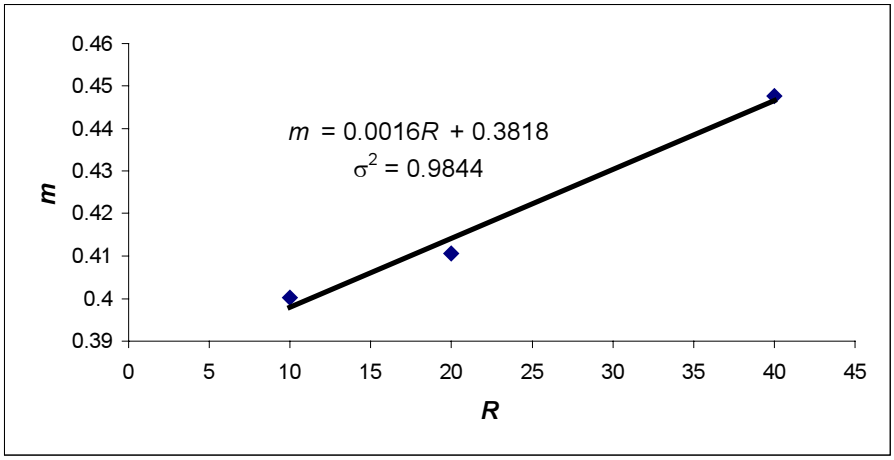

Figure 8. The exponent m vs. the Reynolds number R.

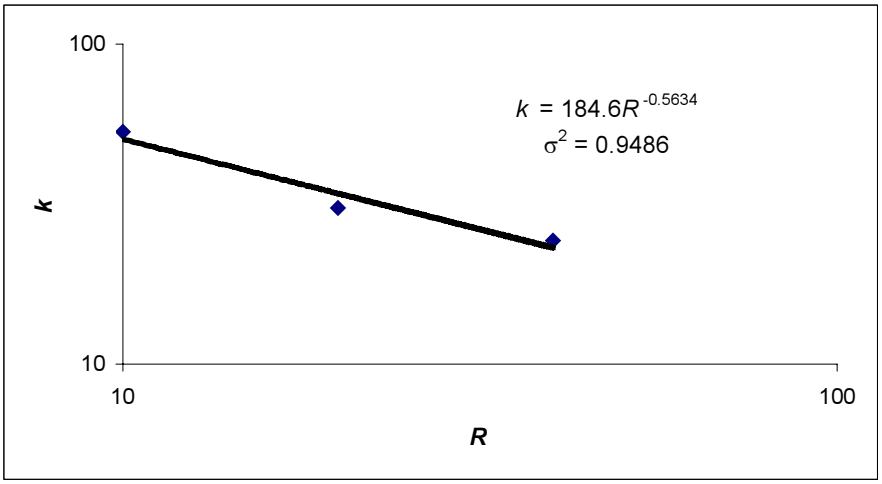

Figure 9. The slope k vs. the Reynolds number R.

We found that *a(R)* and *m(R)* can be fitted with linear function reasonably and power law can give satisfactory fitting for *k*(*R*).

$$a = 0.650R + 12.577\,,\ \ \sigma^2=0.977; \tag{4.14}$$

$$m = 0.0016R + 0.382\,,\ \ \sigma^2=0.984; \tag{4.15}$$

$$k = 184.6R^{-0.563}\,,\ \ \sigma^2=0.949; \tag{4.16}$$

With equations (4.14), (4.15) and (4.16), we can obtain general correlations which apply to the flow with a Reynolds number in the range of 10 – 40.

$$\begin{cases} \boldsymbol{\lambda(y) = (0.650R + 12.577)F(y)^{(0.0016R+0.382)}} \ \text{on the stable branch} \\ \text{of steady solutions away from equilibrium;} \qquad (4.17) \\ \boldsymbol{\lambda(y) = 184.6R^{-0.563}F(y)} \qquad \text{on the stable branch} \\ \text{of steady solutions through equilibrium.} \qquad (4.18) \end{cases}$$

The correlations give us analytical expressions for the lift force. To compare to the analytical lift force expressions in the literature, we use the dimensional forms of $\lambda(y)$ and $F(y)$ in (4.17) and (4.18). After arrangement, the equations are in the following form:

$$\begin{cases} L = \dfrac{(0.650R + 12.577)\pi}{4}\eta v^{-0.0032R + 0.236}\left[U_s(\Omega_s - \Omega_{se})\right]^{0.0016R + 0.382} d^{0.0048R + 0.146} \\ \qquad \text{on the stable branch of steady solutions away from equilibrium;} \qquad (4.19) \\ L = 46.15R^{-0.563}\rho_f U_s(\Omega_s - \Omega_{se})d^2 \\ \qquad \text{on the stable branch of steady solutions through equilibrium.} \qquad (4.20) \end{cases}$$

Equations (4.19) and (4.20), while apply to two-dimensional motion of a particle in a Poiseuille flow, may be compared to well-known lift expressions for a particle in a linear shear flow with shear rate $\dot{\gamma}$. The comparisons are at best tentative because the linear shear neglects the effects of shear gradients and because the lift expressions in linear shear flows are for indefinitely small Reynolds number perturbing Stokes flow on an unbounded domain. Bretherton (1962) found the lift per unit length on a cylinder (2D sphere) at small values of $R = \dot{\gamma}a^2/\nu$ is given by:

$$L = \frac{21.16\eta U_s}{(0.679 - \ln(\sqrt{R/4}))^2 + 0.634} \qquad (4.21)$$

Saffman's (1965) gave expression for the lift on a sphere in a linear shear flow

$$L = 6.46\rho_f^{0.5}\eta^{0.5}U_s\dot{\gamma}^{0.5}a^2 + \text{lower order terms} \qquad (4.22)$$

where a is the radius of the sphere. The lower order terms are:

$$-U_s\, a^3\rho_f\left[\pi\,\Omega_s - \left(\pi - \tfrac{22}{8}\right)\tfrac{1}{2}\dot{\gamma}\right]. \qquad (4.23)$$

For a neutrally buoyant particle at equilibrium, $L = 0$ and from (4.21) and (4.22), $U_s = 0$. The Bretherton and Saffman formulae thus predict that the slip velocity is zero for a neutrally buoyant particle at equilibrium in an unbounded linear shear flow. Patankar *et al.* (2001a) stated that the zero slip velocity is always one solution for a neutrally buoyant particle freely moving in an unbounded linear shear flow, but it may not be the only solution and it can be unstable under certain conditions not yet understood. Feng, Hu and Joseph (1994) showed that a neutrally buoyant particle migrates to the centerline in a Couette flow where $U_s = 0$. Ho and Leal (1974) found a neutrally buoyant sphere equilibrates at the centerline in a Couette flow. The difference is that Feng *et al.* (1994) studied 2D particles in flows at finite Reynolds numbers; while Ho and Leal (1974) studied 3D spheres in flows at indefinitely small Reynolds numbers. From our simulations for 2D Poiseuille flows, $U_s \neq 0$ at the equilibrium position of a neutrally buoyant particle (see figure 4); whereas $\Omega_s = \Omega_{se}$ at equilibrium gives rise to zero lift.

We find that our expression for the lift on the stable branch of steady solutions through equilibrium (4.20) is similar to the higher order term in Saffman's expression for the lift. If we make following changes in equation (4.20): $R = \frac{\rho_f \dot{\gamma}_w d^2}{\eta} \rightarrow R = \frac{\rho_f \dot{\gamma} d^2}{\eta}$, the power of R (-0.563) $\rightarrow$ (-0.5), and use $d = 2a$, equation (4.20) becomes:

$$L = 92.3 \rho_f^{0.5} \eta^{0.5} U_s \dot{\gamma}^{-0.5} (\Omega_s - \Omega_{se}) a \tag{4.24}$$

Comparing equation (4.24) and the leading term in (4.22), we note that both expressions are linear in U_s; both have a similar dependence on ρ_f, η, and a after noting that (4.24) is for the lift force per unit length; but the dependence on $\dot{\gamma}$ and Ω_p is greatly different.

Another formula for the lift on a particle in an inviscid fluid in which uniform motion is perturbed by a weak shear was derived by Auton (1987) and a more recent satisfying derivation of the same result was given by Drew and Passman (1999). They find that

$$L = \frac{2}{3} \pi a^3 \rho \boldsymbol{\omega} \wedge (\mathbf{u} - \mathbf{U}) . \tag{4.25}$$

In plane flow $\boldsymbol{\omega} = \mathbf{e}_z \dot{\gamma}$, $(\mathbf{u} - \mathbf{U}) = \mathbf{e}_x (u - U)$, we have:

$$L = -\frac{4}{3} \pi a^3 \rho \Omega_f (u - U) \mathbf{e}_y \tag{4.26}$$

where $2\Omega_f = -\dot{\gamma}$.

(4.20) and (4.26) have the similar form. Suppose our correlations can be extended to higher Reynolds number, then equation (4.20) reduces to the following form at R = 6358.6:

$$L = \frac{4}{3} \pi a^2 \rho_f U_s (\Omega_s - \Omega_{se}) \tag{4.27}$$

Note that (4.26) is for three-dimensional spheres, whereas our correlation is for two-dimensional particles. Therefore, the same constant in (4.26) and (4.27) can only qualitatively demonstrate that our correlation (4.20) at high Reynolds number can match Auton's expression (4.26) which is for inviscid fluid. The key difference between our correlation and Auton's expression is that we use Ω_s - Ω_{se} in (4.27), in contrast to Ω_f in (4.26)

The correlations prove that the lift force L is determined by the relative motion between the particle and its surrounding fluid. The relative motion can be characterized by the slip velocity U_s

and the angular slip velocity discrepancy Ω_s - Ω_{se}. We emphasize that the relative angular motion is characterized by Ω_s - Ω_{se} rather than Ω_s. Note that Ω_s is always positive at any position in the channel, because normally the angular velocity of the particle does not exceed the angular velocity of the fluid. Therefore, Ω_s can not account for the negative lift force appearing on the stable branch of steady solutions through equilibrium (see figure 4). By using Ω_s - Ω_{se}, we are able to account for the negative lift force. Our correlations cover the whole range from the wall to the centerline except the unstable regions. We believe that our correlations capture the essence of the mechanism of the lift force.

4.2 Correlations with the multi-equilibrium positions of a heavier-than-fluid particle as the references

Under certain conditions, two stable equilibrium positions exist for a heavier-than-fluid particle, one on the stable branch of steady solutionss near the wall, and the other on the stable branch of steady solutionss near the centerline. At the two equilibrium positions (the superscript is for "heavy"):

$$y = y_{e1}^H,\ \Omega_s(y_{e1}^H) = \Omega_{se1}^H,\ \mathsf{L}(y_{e1}^H) = L(y_{e1}^H) - (\rho_p - \rho_f)gd^2\pi/4 = 0;$$

$$y = y_{e2}^H,\ \Omega_s(y_{e2}^H) = \Omega_{se2}^H,\ \mathsf{L}(y_{e2}^H) = L(y_{e2}^H) - (\rho_p - \rho_f)gd^2\pi/4 = 0.$$

On the stable branch near the wall, across y_{e1}^H, $\Omega_s(y) - \Omega_{se1}^H$ and $\mathsf{L}(y)$ change sign; on the stable branch near the centerline, across y_{e2}^H, $\Omega_s(y) - \Omega_{se2}^H$ and $\mathsf{L}(y)$ change sign. Hence, in this section, we will refer the stable branch near the wall as the stable branch of steady solutions through the first equilibrium position, and the stable branch near the centerline as the stable branch of steady solutions through the second equilibrium position. Following is an example to illustrate the change of sign of $\Omega_s(y) - \Omega_{se}^H$ and $\mathsf{L}(y)$ in the case of multi-equilibrium positions.

In the two-dimensional Poiseuille flow with R = 20, a particle with ρ_p=1.016ρ_f has two stable equilibrium positions. The net force:

$$\mathsf{L}(y) = L(y) - (\rho_p - \rho_f)gd^2\pi/4 = L(y) - 12.33.$$

On the stable branch of steady solutions through the first equilibrium position, y_{e1}^H =1.093cm, Ω_{se1}^H =1.5765s^{-1}. In the following table, we list the lift force L, the net force L, the angular slip

velocity Ω_s, the discrepancy $\Omega_s - \Omega_{se1}^H$, $F(y)$ and $\lambda(y)$ for seven points on the stable branch of steady solutions through the first equilibrium position.

y(cm)	L(dyn/cm)	L(dyn/cm)	Ω_s (s^{-1})	$\Omega_s - \Omega_{se1}^H$ (s^{-1})	F(y)	λ(y)
0.55	70.14	57.81	4.77	3.2	11.963	73.609
0.6	55.01	42.68	3.73	2.15	5.717	54.345
0.75	34.54	22.21	2.33	0.753	0.987	28.282
0.9	22.41	10.08	1.8	0.225	0.164	12.837
1	16.46	4.13	1.65	0.073	0.034	5.262
1.15	10.62	-1.71	1.57	-0.00899	-0.002	-2.174
1.25	8.51	-3.82	1.57	-0.00364	-0.0002	-4.861

Table 2. The lift force L, the net force L, the angular slip velocity Ω_s the discrepancy $\Omega_s - \Omega_{se1}^H$, F(y) and λ(y) for seven points on the stable branch of steady solutions through the first equilibrium position (R = 20 and ρ_p=1.016ρ_f). It can be seen that across y_{e1}^H=1.093cm, $\Omega_s(y) - \Omega_{se1}^H$ and L(y) change sign.

On the stable branch of steady solutions through the second equilibrium position, y_{e2}^H=2.377cm, Ω_{se2}^H=1.1837s^{-1}. In the following table, we list the lift force L, the net force L, the slip velocity Ω_s, the discrepancy $\Omega_s - \Omega_{se2}^H$, $F(y)$ and $\lambda(y)$for eight points on the stable branch of steady solutions through the second equilibrium position.

y(cm)	L(dyn/cm)	L(dyn/cm)	Ω_s (s^{-1})	$\Omega_s - \Omega_{se2}^H$ (s^{-1})	F(y)	λ(y)
2	14.470	2.142	1.431	0.247	0.091	2.728
2.25	13.020	0.692	1.266	0.083	0.043	0.882
2.5	11.490	-0.838	1.113	-0.071	-0.039	-1.066
3	8.640	-3.688	0.855	-0.329	-0.176	-4.695
3.5	6.043	-6.285	0.619	-0.564	-0.298	-8.002
4	3.047	-9.281	0.402	-0.782	-0.413	-11.816
4.5	0.188	-12.139	0.221	-0.963	-0.447	-15.456
5	-1.521	-13.849	0.105	-1.079	-0.386	-17.633

Table 3. The lift force L, the net force L, the angular slip velocity Ω_s, the discrepancy $\Omega_s - \Omega_{se2}^H$, F(y) and λ(y) for eight points on the stable branch of steady solutions through the second equilibrium position (R = 20 and ρ_p=1.016ρ_f). It can be seen that across y_{e2}^H=2.377cm, $\Omega_s(y) - \Omega_{se2}^H$ and L(y) change sign.

From table 2 and 3, it can be seen that for a heavier-than-fluid particle with two stable equilibrium positions, the discrepancy $\Omega_s(y) - \Omega_{se}^H$ changes sign across either of the two positions and correlates very well with the net force L(y).

Correlations will now be derived on the two stable branches. On the stable branch of steady solutions through the first equilibrium position, the equilibrium position y_{e1}^H is taken as the reference position and Ω_{se1}^H is used to compute the discrepancy. The dimensionless parameters are in the following form:

$$\lambda(y) = \frac{4\rho_f d\left[L(y) - (\rho_p - \rho_f)g\pi d^2/4\right]}{\pi\eta^2} \text{ and } F(y) = \frac{\rho_f^2 U_s(y)\left[\Omega_s(y) - \Omega_{se1}^H\right]d^3}{\eta^2}.$$

We present the correlations for two cases, ρ_p=1.016ρ_f and R =20; ρ_p=1.045ρ_f and R =40. For the case with ρ_p=1.016ρ_f and R=20, y_{e1}^H = 1.093cm, Ω_{se1}^H =1.5765s^{-1}; for the case with ρ_p=1.045ρ_f and R=40, y_{e1}^H = 0.9476cm, Ω_{se1}^H =4.332s^{-1}.When $y < y_{e1}^H$ on the stable branch of steady solutions through the first equilibrium position, $\Omega_s(y) - \Omega_{se1}^H$ and L(y) are positive, so are λ(y) and F(y). We find that the correlation between the positive λ(y) and F(y) is still a power law. In figure 10, λ(y) vs. F(y) for y < y_{e1}^H on the stable branch of steady solutions through the first equilibrium position is plotted. It can be seen that power laws fit the data well. When y > y_{e1}^H on the stable branch through the first equilibrium position, $\Omega_s(y) - \Omega_{se1}^H$ and L(y) are negative, so are λ(y) and F(y). We have not found a way to correlate the negative λ(y) and F(y).

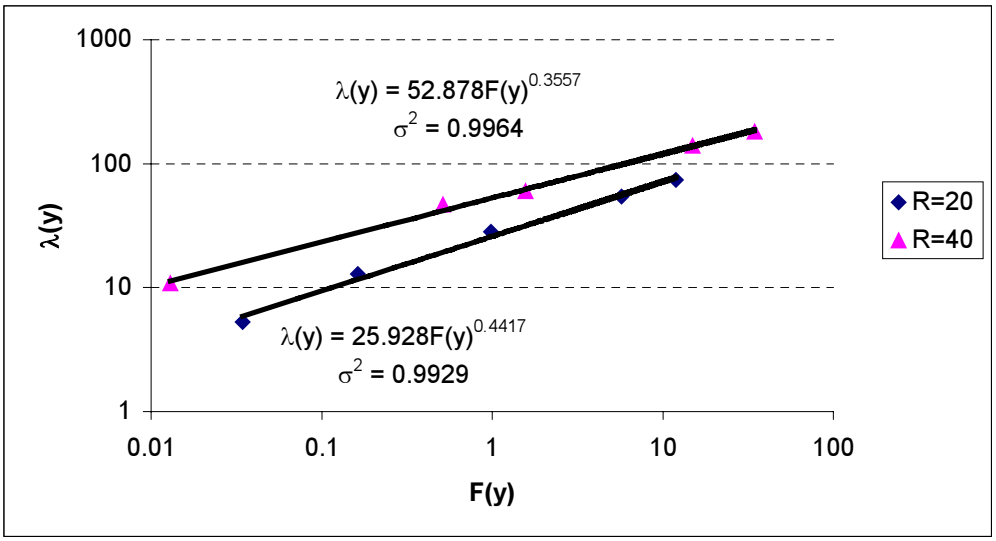

Figure 10. The positive λ(y) vs. F(y) for y < y_{e1}^H on the stable branch of steady solutions through the first equilibrium position. Two cases are plotted, ρ_p=1.016ρ_f and R =20 (see table 2); ρ_p=1.045ρ_f and R =40. For the case with ρ_p=1.016ρ_f and R =20, y_{e1}^H = 1.093cm, Ω_{se1}^H = 1.5765s^{-1}; for the case with ρ_p=1.045ρ_f and R =40, y_{e1}^H = 0.9476cm, Ω_{se1}^H =4.332s^{-1}. When y < y_{e1}^H, λ(y) and F(y) are positive and can be fitted with power laws.

The correlations between the positive λ(y) and F(y) for y < y_{e1}^H on the stable branch of steady solutions through the first equilibrium position are listed as following:

$$\lambda(y) = 25.93F(y)^{0.442}, \sigma^2 = 0.993, \text{ for } \rho_p=1.016\rho_f \text{ and } R=20; \tag{4.28}$$

$$\lambda(y) = 52.88F(y)^{0.356}, \sigma^2 = 0.996, \text{ for } \rho_p=1.045\rho_f \text{ and } R=40. \tag{4.29}$$

On the stable branch of steady solutions through the second equilibrium position, the equilibrium position y_{e2}^H is taken as the reference position and Ω_{se2}^H is used to compute the discrepancy. The dimensionless parameters are in the following form:

$$\lambda(y) = \frac{4\rho_f d\left[L(y) - (\rho_p - \rho_f)g\pi d^2/4\right]}{\pi\eta^2} \text{ and } F(y) = \frac{\rho_f^2 U_s(y)\left[\Omega_s(y) - \Omega_{se2}^H\right]d^3}{\eta^2}.$$

We find that the correlation between λ(y) and F(y) is still a linear equation. We present the correlations for two cases, ρ_p=1.016ρ_f and R =20; ρ_p=1.045ρ_f and R =40. For the case with ρ_p=1.016ρ_f and R=20, y_{e2}^H = 2.377cm, Ω_{se2}^H=1.1837s^{-1}; for the case with ρ_p=1.045ρ_f and R=40, y_{e2}^H = 2.705cm, Ω_{se2}^H=2.737s^{-1}. Figure 11 shows λ(y) vs. F(y) on the stable branch of steady solutions through the second equilibrium position and the linear fitting.

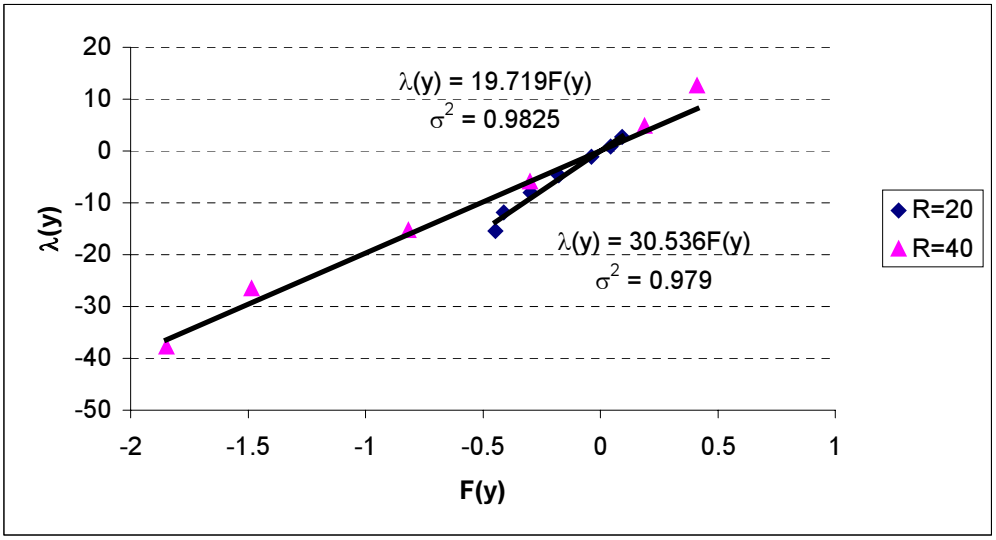

Figure 11. λ(y) vs. F(y) on the stable branch of steady solutions through the second equilibrium position for two cases, ρ_p=1.016ρ_f and R =20 (see table 3); ρ_p=1.045ρ_f and R =40. For the case with ρ_p=1.016ρ_f and R=20, y_{e2}^H = 2.377cm, Ω_{se2}^H = 1.1837s^{-1}; for the case with ρ_p=1.045ρ_f and R=40, y_{e2}^H = 2.705cm, Ω_{se2}^H =2.737s^{-1}. Linear correlations give satisfactory fitting for the λ(y) vs. F(y) curves.

The linear correlations between λ(y) and $F(y)$ on the stable branch of steady solutions through the second equilibrium position are listed as following:

$$\lambda(y) = 30.54F(y)\text{, } \sigma^2 = 0.979\text{, for } \rho_p=1.016\rho_f \text{ and } R=20; \tag{4.30}$$

$$\lambda(y) = 19.72F(y)\text{, } \sigma^2 = 0.983\text{, for } \rho_p=1.045\rho_f \text{ and } R=40. \tag{4.31}$$

The correlations derived with multi-equilibrium positions of a heavier-than-fluid particle as reference positions can be compared to the correlations with the single equilibrium position as the reference position.

	stable branch near the wall	stable branch near the centerline
R=20, with the single equilibrium position of a neutrally buoyant particle as the reference position	$\lambda(y) = 27.29F(y)^{0.411}$	$\lambda(y) = 30.74F(y)$
R=20, with multi-equilibrium positions of a	$\lambda(y) = 25.93F(y)^{0.442}$	$\lambda(y) = 30.54F(y)$

heavier-than-fluid particle as reference positions		
R=40, with the single equilibrium position of a neutrally buoyant particle as the reference position	$\lambda(y) = 38.01F(y)^{0.448}$	$\lambda(y) = 24.35F(y)$
R=40, with multi-equilibrium positions of a heavier-than-fluid particle as reference positions	$\lambda(y) = 52.88F(y)^{0.356}$	$\lambda(y) = 19.72F(y)$

Table 4. The comparison between the correlations derived with the single equilibrium position of a neutrally buoyant particle as the reference position and the correlations with multi-equilibrium positions of a heavier-than-fluid particle as reference positions.

From table 4, we can see that the form of the correlations is a power law on the stable branch of steady solutions near the wall and a linear equation on the stable branch of steady solutions near the centerline, which is independent of the choice of the reference position. However, the coefficients in the correlations do depend on the reference positions. We have not found quantitative relations between the coefficients of the correlations with different reference positions.

5.Conclusions

The focus of the present paper is the lift force on a circular particle in a 2D Poiseuille flow. It is known that certain region in a channel is unstable and a particle can not equilibrate in an unstable region. For example, Ho and Leal (1974) pointed out the centerline is an unstable equilibrium position in a 2D Poiseuille flow. By constrained simulation, we are able to determine the stable and unstable regions by examining the L vs. y curve. The domain from the wall to the centerline can be divided into four regions with the following order: wall – stable – unstable – stable – unstable – centerline.

The lift force L on a particle is determined by the relative motion between the particle and its surrounding fluid. The relative motion can be characterized by the slip velocity U_s and the angular slip velocity discrepancy Ω_s - Ω_{se}. For neutrally buoyant and heavier-than-fluid particles, following relation between Ω_s -Ω_{se} and L exist: Ω_s -Ω_{se}<0 when the particle is above the equilibrium position; Ω_s -Ω_{se}>0 when the particle is below the equilibrium position. With a stable equilibrium as the reference state, negative Ω_s -Ω_{se} leads to negative L, positive Ω_s -Ω_{se} leads to

positive L; with an unstable equilibrium position as the reference state, negative Ω_s -Ω_{se} leads to positive L, positive Ω_s -Ω_{se} leads negative L.

Correlations between L and the product of U_s and Ω_s - Ω_{se} are obtained on the two stable branches of steady solutions. Using dimensionless parameters R_{Gy} and $(R_{Uy} \cdot R_{\Omega y})$, the correlation is a power law on the stable branch of steady solutions near the wall and a linear relation (which can be taken as a power law with the power of one) on the stable branch of steady solutions near the centerline. Two forms of the correlations are presented, one with the single equilibrium position of a neutrally buoyant particle as the reference, the other with the multi-equilibrium positions of a heavier-than-fluid particle as the references. The power law correlations reveal the self-similar property in the flow of dispersed matter which is not evident from the equations of motion.

Acknowledgement

This work was partially supported by the National Science Foundation KDI/New Computational Challenge grant (NSF/CTS-98-73236); by the US Army, Mathematics; by the DOE, Engineering Research Program of the Office of Basic Energy Sciences; by a grant from the Schlumberger foundation; from STIM-LAB Inc.; and by the Minnesota Supercomputer Institute.

References:

Asmolov, E. S. 1999 The inertial lift on a spherical particle in a plane Poiseuille flow at large channel Reynolds number. *J. Fluid Mech.* **381**, 63-87.

Auton, T. R. 1987 The lift force on a spherical body in a rotational flow, *J. Fluid Mech.* **183**, 199-218.

Barenblatt, G. I., 1996. *Scaling, Self Similarity and Intermediate Asymptotics*. Cambridge Univ. Press.

Bretherton, F. P. 1962 Slow viscous motion round a cylinder in a simple shear. *J. Fluid Mech.* **12**, 591-613.

Choi H. G. and Joseph, D. D. 2001 Fluidization by lift of 300 circular particles in plane Poiseuille flow by direct numerical simulation, *J. Fluid Mech*. **438**, July, 101-128.

Drew, D. A. and Passman S. 1999 *Theory of Multicomponent Fluids*, Springer.

Feng, J., Hu, H. H. and Joseph, D. D. 1994 Direct simulation of initial values problems for the motion of solid bodies in a Newtonian fluid. Part 2: Couette and Poiseuille flows. *J. Fluid Mech.* **277**, 271-301.

Ho, B. P. and Leal, L. G. 1974 Inertial migration of rigid spheres in two-dimensional unidirectional flows, *J. Fluid Mech*. **65**, 365-400.

Joseph, D. D. 2000 *Interrogations of Direct Numerical Simulation of Solid-Liquid Flow*, to appear, see also *http://www.aem.umn.edu/people/faculty/joseph/interrogation.html*.

Joseph, D. D. and Ocando, D. Slip Velocity and Lift, 2002, *J. Fluid Mech*. **454**, 263-286

McLaughlin, J.B. 1991 Inertial migration of a small sphere in linear shear flows, *J. Fluid Mech*. **224**, 261-274.

Patankar, N.A., Huang, P.Y., Ko, T. and Joseph, D. D. 2001a. Lift-off of a single particle in Newtonian and viscoelastic fluids by direct numerical simulation, *J. Fluid Mech.*, **438**, 67-100.

Patankar, N. A., Ko, T., Choi H. G. and D.D. Joseph, 2001b. A correlation for the lift-off of many particles in plan Poiseuille of Newtonian fluids, *J. Fluid Mech*. **445**, 55-76.

Patankar, N. A., Joseph, D.D., Wang, J., Barree, R.D., Conway, M., and Asadi, M., 2002 Power law correlations for sediment transport in pressure driven channel flows, *Int. J. Multiphase Flow*, to appear.

Richardson J. F. and Zaki, W. N. 1954. Sedimentation and Fluidization: Part I, *Trans. Instn. Chem. Engrs*. **32**, 35–53.

Saffman, P. G. 1965 The lift on a small sphere in a slow shear flow, *J. Fluid Mech.* **22**, 385; and Corrigendum, *J. Fluid Mech*. 31, 624 (1968).

Schonberg, J. A. and Hinch E. J. 1989 Inertial migration of a sphere in Poiseuille flow, *J. Fluid Mech*. **203**, 517-524.

Segrè G. and Silberberg, A. 1961 Radial Poiseuille flow of suspensions, *Nature,* **189**, 209.

Segrè G. and Silberberg, A. 1962 Behavior of macroscopic rigid spheres in Poiseuille flow, Part I, *J. Fluid Mech.,* **14**, 115-135.

Vasseur, P. and Cox, R.G. 1976 The lateral migration of a spherical particle in two-dimensional shear flows, *J. Fluid Mech.* **78**, 385-413.

Wang, J., Joseph, D. D., Patankar, N. A., Conway, M. and Barree, R. D. 2002 Bi-power law correlations for sediment transport in pressure driven channel flows, submitted to *Int. J. Multiphase Flow*.